Supporting Information for

A Selective Suppression of Stimulated Raman Scattering with Another Competing Stimulated Raman Scattering

Doyeon Kim[1,2], Dae Sik Choi[3,4], Jiwoong Kwon[1,2], Sang-Hee Shim[1,2,] Hanju Rhee[5,*], and Minhaeng Cho[1,2,*]*

[1]Center for Molecular Spectroscopy and Dynamics, Institute for Basic Science (IBS), Seoul 02841, Republic of Korea.

[2]Department of Chemistry, Korea University, Seoul 02841, Republic of Korea.

[3]Technology Human Resource Support for SMEs Center, Korea Institute of Industrial Technology (KITECH), Cheonan, 31056, Republic of Korea.

[4]Research Institute, Smart Korea, Daejeon, 34141, Republic of Korea.

[5]Seoul Center, Korea Basic Science Institute, Seoul 02841, Republic of Korea.

* E-mails: sangheeshim@korea.ac.kr (S-H.S.), hjrhee@kbsi.re.kr (H.R.), or mcho@korea.ac.rk (M.C.)

Supplementary Notes

I. Theoretical Description of Three-beam SRS Processes

Since a detailed theory on the three-beam double SRS was presented elsewhere by one of the authors,[S1] here we shall present a brief description of three-beam parallel SRS processes in terms of incident beam intensities in the sample.

I-A. Two-beam SRS

In conventional two-beam SRS spectroscopy or microscopy, two laser beams are used and called Raman pump and Stokes, where the frequency of the pump, ω_p, is higher than that of the Stokes beam, ω_s. When $\omega_p - \omega_s = \omega_v$, where ω_v denotes the frequency of a Raman-active mode, the SRS is resonantly enhanced.[S2,S3] In the present work, this target Raman mode is the ring breathing mode of benzene of which frequency is 992 cm^{-1}. In the presence of two electric fields, there is an oscillating component with frequency of $\omega = \omega_p - \omega_s$, which essentially drives the resonant molecular vibration. Consequently, the stimulated molecular vibrations modulate the refractive index of the material, which scatters Stokes beam to generate a third-order stimulated Raman scattering field at the pump field frequency, which in turn interfere with the pump itself resulting in a pump beam attenuation, i.e., Raman loss. Each individual SRS involves not only an annihilation of a pump photon but also simultaneous creations of both Stokes photon and molecular oscillation.

For two-beam SRS, the effective radiation-matter interaction Hamiltonian can be written as

$$\hat{H}_{int} = -\left(\frac{\partial \alpha}{\partial q}\right)_0 \frac{\hbar^{3/2}}{2V}\sqrt{\frac{1}{Nm\varepsilon_s\varepsilon_p}}\sqrt{\frac{\omega_s\omega_p}{2\omega_v}}$$

$$\times\left[a_p a_s^+ b^+ e^{i\{(\mathbf{k}_p-\mathbf{k}_s-\mathbf{k}_v)\cdot\mathbf{r}-(\omega_p-\omega_s-\omega_v)t\}} + a_p^+ a_s b e^{-i\{(\mathbf{k}_p-\mathbf{k}_s-\mathbf{k}_v)\cdot\mathbf{r}-(\omega_p-\omega_s-\omega_v)t\}}\right]. \quad \text{(S1)}$$

Here, the first derivative of molecular polarizability, α, with respect to vibrational coordinate, q, corresponds to the transition polarizability tensor, which will be treated as a scalar for the sake of simplicity. In Eq.(S1), V is the interaction volume, N is the number of molecules in the interaction volume, m is the reduced mass of the molecular vibration, and ω_v is frequency. ε_p and ε_s are the permittivities of the material at the pump and Stokes frequencies, respectively. a and a^+ are the annihilation and creation operators, respectively, of the photons in the Stokes or the pump field. The creation and annihilation operators of each molecular oscillator are denoted as b^+ and b, respectively. In addition, $\mathbf{k}$ in Eq.(S1) is the corresponding wave vector. In the approximate interaction Hamiltonian given in Eq.(S1), all the highly oscillating field components that do not participate in the vibrationally resonant Raman scattering processes are ignored. Due to the energy and moment conservation principles, the following two equalities, $\omega_p = \omega_s + \omega_v$ and $\mathbf{k}_p = \mathbf{k}_s + \mathbf{k}_v$, should be satisfied for the SRS process.

Using the interaction Hamiltonian (Eq.(S1)) and the Fermi golden rule expression for transition rate calculation, one can obtain the net rate of change in the Stokes photon number per unit length, which is the difference between the emission and absorption rates of the Stokes beam. Considering the phase velocity of the Stokes beam in the material, which is $v_s = c/\sqrt{\varepsilon_s/\varepsilon_0}$, one can find that the rate equation for the Stokes photon number per unit length n_s with respect to the z coordinate parallel to the beam propagation direction is given by

$$\frac{dn_s(z)}{dz} = \left| \left(\frac{\partial \alpha}{\partial q} \right)_0 \right|^2 \frac{\pi \hbar^2}{4V^2 Nm\,\varepsilon_s \varepsilon_p v} \frac{\omega_p \omega_s}{\omega_v} \left\{ n_s(n_v+1)n_p + (n_v+1)n_p - n_s n_v n_p - n_s n_v \right\} \rho(\hbar\omega_f) \,. \quad \text{(S2)}$$

where $\rho(\hbar\omega_f)$ denotes the density of final states, which is often modelled as a Lorentzian function. The differential equation for the pump photon number n_p that is also a function of z along the beam propagation direction is related to that of the Stokes photon number in Eq.(S2) as $dn_s(z)/dz = -dn_p(z)/dz$. The rate equation for $n_s(z)$ in Eq.(S2) consists of stimulated emission, spontaneous emission, stimulated absorption, and spontaneous absorption. However, not only because typical vibrational energy is much larger than the thermal energy, $k_B T$, at room temperature but also because the average photon number of the incident Stokes beam is much larger than one, it is safe to ignore the spontaneous emission contribution to the Stokes Raman gain signal. As a result, the rate equation in Eq.(S2) can be simplified as

$$\frac{dn_s(z)}{dz} = G_s(\omega_p, \omega_s, \omega_v) n_p(z) n_s(z) \,, \tag{S3}$$

where the auxiliary constant G_s is defined as

$$G_s(\omega_p, \omega_s, \omega_v) = \left| \left(\frac{\partial \alpha}{\partial q} \right)_0 \right|^2 \frac{\pi \hbar^2}{4V^2 Nm\, \varepsilon_s \varepsilon_p v_s} \frac{\omega_p \omega_s}{\omega_v} \rho(\hbar \omega_f) \,. \tag{S4}$$

The constant G_s is related to the well-known gain coefficient g if the above differential equation (S3) is rewritten in terms of beam intensities instead of photon numbers, i.e.,

$$\frac{dI_s(z)}{dz} = \frac{\mu_p V G_s(\omega_p, \omega_s, \omega_v)}{\hbar \omega_p c} I_p(z) I_s(z) = g(\omega_p, \omega_s, \omega_v) I_p(z) I_s(z) \,, \tag{S5}$$

where μ is the refractive index of the material. Now, defining the increased amount of Stokes photon number due to the stimulated Raman process as $\Delta n_s(z) = n_s(z) - n_s(z=0)$ and denoting the Stokes gain signal intensity as $\Delta I_s(z) = \left(\hbar \omega_s c / \mu_s V \right) \Delta n_s(z)$, we have

$$\frac{d\Delta I_s(z)}{dz} = G_s \left\{ \frac{\mu_p V}{\hbar \omega_p c} I_p(0) I_s(0) + \left[\frac{\mu_p V}{\hbar \omega_p c} I_p(0) - \frac{\mu_s V}{\hbar \omega_s c} I_s(0) \right] \Delta I_s(z) - \frac{\mu_s V}{\hbar \omega_s c} \Delta I_s^2(z) \right\} \tag{S6}$$

The general solution of the above differential equation is well-known.[S1-S3]

In the limiting case that the incident pump and Stokes beam intensities are weak or the Raman gain coefficient is small, one can ignore the linear and quadratic (in $\Delta I_s(z)$) terms on the right-hand side of the differential equation (S6). Then, the increased Stokes gain signal intensity at the rear boundary ($z = L$) of the sample (material) is simply given as

$$\Delta I_s(L) = \frac{\hbar \omega_s c}{\mu_s V} \Delta n_s(L) = \frac{\mu_p V}{\hbar \omega_p c} G_s I_p(0) I_s(0) L = g I_p(0) I_s(0) L \,. \tag{S7}$$

Usually, the SRS spectroscopy or imaging studies are performed in this weak field limit.[S4,S5] However, as the beam intensities increase, the Stokes Raman gain signal increases exponentially with respect to z and eventually reaches the saturation limit where all the high-energy pump photons are converted into the low-energy Stokes photons with an equal number of vibrational excitations in the material.

I-B. Three-beam double SRS

Now, let us consider the case that there is an additional Raman-active mode with frequency of $\omega_{v'}$ in the same molecules that can be excited via another SRS process induced by the third beam with frequency of ω_d satisfying $\omega_{v'} = \omega_p - \omega_d$. In this paper, it is the C-H stretch mode of benzene of which frequency is 3056 cm^{-1}. Thus, we have that $\omega_p > \omega_s > \omega_d$. In fact, this third beam is nothing but another Stokes beam. However, as will be shown below experimentally, it can be used to deplete the Raman pump beam to eventually suppress the SRS signal associated with the target mode with frequency of ω_v. Thus, we shall call the third (Stokes 2) beam as *depletion* beam and the corresponding Raman mode will be referred to as depletion Raman mode throughout this paper.

For the three-beam geometry, there are three difference-frequency field components oscillating at $\omega_p - \omega_s$, $\omega_p - \omega_d$, and $\omega_s - \omega_d$. Here, we deliberately choose the two Raman modes and the frequencies of pump, Stokes, and depletion beams so that there is no Raman-active mode of which frequency is $\omega_s - \omega_d$ (Fig. 1d). Then, the *p-s* (pump-and-Stokes) and *p-d* (pump-and-depletion) SRS processes occur and compete with each other for the same pump photons. The rate equations for the increased photon numbers of the Stokes and depletion beams, which are denoted as $\delta n_s(z)$ and $\delta n_d(z)$, respectively, can be obtained by using the interaction Hamiltonian and Fermi gold rule expression.[S1] The two differential equations for the increased intensities of the Stokes and depletion beams are given as[1]

$$\frac{d\Delta I_s(z)}{dz} = G_s\left(\frac{\mu_p V}{\hbar\omega_p c} I_p(0) - \frac{\mu_s V}{\hbar\omega_s c}\Delta I_s(z) - \frac{\mu_d V}{\hbar\omega_d c}\Delta I_d(z)\right)\left(I_s(0) + \Delta I_s(z)\right) \tag{S8}$$

$$\frac{d\Delta I_d(z)}{dz} = G_d\left(\frac{\mu_p V}{\hbar\omega_p c} I_p(0) - \frac{\mu_s V}{\hbar\omega_s c}\Delta I_s(z) - \frac{\mu_d V}{\hbar\omega_d c}\Delta I_d(z)\right)\left(I_d(0) + \Delta I_d(z)\right), \tag{S9}$$

where the coefficient $G_d(\omega_p, \omega_d, \omega_{v'})$ is related to the gain coefficient of the stimulated Raman scattering by the vibrationally excited $\omega_{v'}$-mode and it is similarly defined as

$$G_d(\omega_p, \omega_d, \omega_{v'}) = \left| \left(\frac{\partial \alpha}{\partial q'} \right)_0 \right|^2 \frac{\pi \hbar^2}{4V^2 N m' \varepsilon_d \varepsilon_p v_d} \frac{\omega_p \omega_d}{\omega_{v'}} \rho(\hbar \omega_{f'}) . \tag{S10}$$

The rate equation for the photon number of the pump beam in this case can be obtained from Eqs. (S8) and (S9) with the corresponding Manley-Rowe relation for the present three-beam double SRS processes. That is to say, we have

$$dn_p(z)/dz = -(dn_s(z)/dz + dn_d(z)/dz) \tag{S11}$$

The two differential equations in Eqs. (S8) and (S9) are coupled with each other and it is not possible to obtain a mathematically exact solution for the increased intensities of the Stokes and depletion beams. Nonetheless, it is straightforward to carry out numerical simulations (see Ref.[S1] for details). Furthermore, approximate solutions for a few limiting cases were found and shown to be of use to understand the underlying mechanism of selective suppression of one SRS process by using competing SRS process.

The coupled rate equations in Eqs. (S8) and (S9) are similar to the chemical kinetic equations of a special kind of branching chemical reactions, where both reactions involve the same reactant denoted as *P*. *P* reacts with either *S* or *D* and both reactions are second-order bimolecular processes with rate constants proportional to G_s and G_d, respectively. Note that the increasing rate of the depletion beam intensity is largely determined by the initial intensity of the depletion beam. As will be shown here in this paper, we could experimentally increase the depletion beam intensity with respect to a fixed Stokes beam intensity, which makes most of the pump photons to be converted into the depletion beam photons with generating an equal number of vibrational excitations on the *q'* mode (C-H stretches of benzene in the present work). Thereby, the suppression of stimulated Raman gain at Stokes frequency is achievable by controlling the relative ratio of the intensity of the depletion beam to that of the Stoke beam.

I-C. Weak Stokes and depletion beams

If the pump beam intensity is much stronger than both Stokes and depletion beam intensities, the net depletion of pump beam is negligible as compared with the initial pump beam intensity. In this limiting case, the gains of Stokes and depletion beams are simply proportional to the interaction distance z and initial beam intensities, i.e.,

$$\Delta I_s(z) \cong \frac{\mu_p V G_s}{\hbar\omega_p c} I_p(0) I_s(0) z \tag{S12}$$

$$\Delta I_d(z) \cong \frac{\mu_p V G_d}{\hbar\omega_p c} I_p(0) I_d(0) z\,. \tag{S13}$$

All the previous multi-color SRS imaging or spectroscopy experiments were performed in this weak field limit.[S4,S5] Therefore, the Raman gain signals in the Stokes and depletion (second Stokes) beams are independent from each other.

I-D. Strong depletion and weak Stokes beams

As demonstrated in the present experimental work, when the intensity of the depletion beam is increased, the Stokes gain becomes coupled with or dependent on the Raman gain or the intensity of the depletion beam in the Raman medium. Let us consider the case that the photon numbers satisfy $n_d(0) > n_p(0) > n_s(0)$, which can be experimentally achievable. Then, the Stokes Raman gain signal, ΔI_s, can be ignored in the rate equations (S8) and (S9), and then the approximate rate equations become

$$\frac{d\Delta I_s(z)}{dz} = G_s I_s(0)\left(\frac{\mu_p V}{\hbar\omega_p c} I_p(0) - \frac{\mu_d V}{\hbar\omega_d c}\Delta I_d(z)\right) \tag{S14}$$

$$\frac{d\Delta I_d(z)}{dz} = G_d\left(\frac{\mu_p V}{\hbar\omega_p c} I_p(0) - \frac{\mu_d V}{\hbar\omega_d c}\Delta I_d(z)\right)\left(I_d(0) + \Delta I_d(z)\right), \tag{S15}$$

The rate equation (S14) shows that the Stokes gain signal is coupled to the gain signal of the depletion beam. After obtaining the solution of Eq.(S15), inserting it into (S14), integrating the resulting differential equation, we find the analytical solution for the Stokes gain signal to be

$$\begin{aligned}\Delta I_s(z) = {} & G_s I_s(0)\left(\frac{\mu_p V}{\hbar\omega_p c} I_p(0) + \frac{\mu_d V}{\hbar\omega_d c} I_d(0)\right) z \\ & + \frac{G_s}{G_d} I_s(0)\left\{\ln\left(\frac{\mu_p \omega_d I_p(0)}{\mu_d \omega_p I_d(0)} + 1\right) - \ln\left(\frac{\mu_p \omega_d I_p(0)}{\mu_d \omega_p I_d(0)} + e^{G_d\left[\frac{\mu_p V}{\hbar\omega_p c} I_p(0) + \frac{\mu_d V}{\hbar\omega_d c} I_d(0)\right] z}\right)\right\}\end{aligned} \tag{S16}$$

The formal expression for the Stokes gain signal in Eq.(S16) is clearly a function of the pump and depletion beam intensities. Albeit complicated, it does provide useful information on the efficiency in suppressing the Stokes gain signal by using another competing SRS process induced by the depletion beam. For the sake of direct comparison with experimental results, let us define the suppression efficiency as the ratio of the difference between Stokes gain signal without and with depletion beam to the Stokes gain signal without depletion beam, i.e.,

$$\eta \equiv \frac{\Delta I_s(z, I_d(0)=0) - \Delta I_s(z, I_d(0))}{\Delta I_s(z, I_d(0)=0)}. \tag{S17}$$

In the limit of zero depletion beam intensity, the suppression efficiency is zero. On the other hand, as the depletion beam intensity increases so that the competing SRS process dominates over the SRS process induced by the Stokes beam, the suppression efficiency approaches unity. From the asymptotic limit of Eq.(S16) when the depletion beam intensity approaches zero, or from Eq.(S12), we have $\Delta I_s(z, I_d(0)=0) = \frac{\mu_p V G_s}{\hbar\omega_p c} I_p(0) I_s(0) z$. Thus, we finally obtain that the suppression efficiency is given by

$$\eta = 1 - \frac{\hbar\omega_p c}{\mu_p V I_p(0) z}\left\{\left(\frac{\mu_p V}{\hbar\omega_p c} I_p(0) + \frac{\mu_d V}{\hbar\omega_d c} I_d(0)\right) z + \frac{1}{G_d} \ln \frac{\left(\frac{\mu_p \omega_d I_p(0)}{\mu_d \omega_p I_d(0)} + 1\right)}{\left(\frac{\mu_p \omega_d I_p(0)}{\mu_d \omega_p I_d(0)} + e^{G_d\left[\frac{\mu_p V}{\hbar\omega_p c} I_p(0) + \frac{\mu_d V}{\hbar\omega_d c} I_d(0)\right] z}\right)}\right\}. \tag{S18}$$

To understand the effect of the depletion beam intensity of the Stokes gain signal, Eq.(S18) can be re-rewritten in terms of photon numbers per unit length as

$$\eta = 1 - \frac{1}{n_p(0) z}\left\{\left(n_p(0) + n_d(0)\right) z + \frac{1}{G_d} \ln \frac{\left(\frac{n_p(0)}{n_d(0)} + 1\right)}{\left(\frac{n_p(0)}{n_d(0)} + e^{G_d\left[n_p(0) + n_d(0)\right] z}\right)}\right\}. \tag{S19}$$

Introducing a dimensionless coordinate ξ defined as $\xi \equiv G_d n_p(0) z$ and denoting the ratio $n_d(0)/n_p(0)$ as *x*, one can re-write Eq.(S19) as

$$\eta = 1 - \left\{ (1+x) + \frac{1}{\xi} \ln\left(\frac{x+1}{x e^{\xi(1+x)} + 1} \right) \right\}. \tag{S20}$$

For a few ξ values, the numerically calculated curves of the suppression factor in Eq.(S20) are presented in Fig. S2. As expected, as the depletion beam intensity increases or the dimensionless coordinate increases, the suppression factor monotonically increases. From the definition of the dimensionless coordinate, ξ, it is clear that as the Raman gain coefficient of the depletion mode, the incident pump intensity (or photon number), and the interaction length increase, one can strongly suppress the target SRS signal. We shall use this theoretical result, Eq.(S20), to quantitatively analyze our experimental data obtained from our three-beam double SRS measurements.

II. Theoretical description of stimulated Raman loss of the pump

As described in Sec.I, the pump photons are annihilated by the two competing SRS processes that are induced by the Stokes and the depletion beams. As the depletion beam intensity increases, more pump photons are put into the SRS process associated with the depletion beam and the depletion mode (C-H stretch), which in turn suppress the target SRS process that creat both Stokes photons and vibrational excitations of the ring breathing mode. To further investigate the underlying mechanism of our three-beam double SRS process, we measured the pump spectra with increasing energy of the depletion beam (Fig. 4a). The maximum value of the pump intensity decays exponentially (with decay constant 114.5 nJ) as the energy of depletion beam increases (Fig. 4c, red). In fact, the theoretical expressions for the Raman gain rates of the Stokes and depletion beams given in Eqs.(S8), (S9), and (S11) can be directly used to obtain the rate of Raman loss of the pump beam. We found that the differential equation of the pump loss is given by[S1]

$$\begin{aligned} -\frac{d\Delta I_p(z)}{dz} &= \left(\frac{\mu_s V G_s I_s(0)}{\hbar\omega_s c} + \frac{\mu_d V G_d I_d(0)}{\hbar\omega_d c} \right) I_p(0) \\ &+ \left(\frac{\mu_s V G_s I_s(0)}{\hbar\omega_s c} + \frac{\mu_d V G_d I_d(0)}{\hbar\omega_d c} - \frac{\mu_p V \bar{G} I_p(0)}{\hbar\omega_p c} \right) \Delta I_p(z) - \frac{\mu_p V}{\hbar\omega_p c} \bar{G} \Delta I_p^2(z) \end{aligned}, \tag{S22}$$

where the mean gain coefficient $\bar{G}$ is defined as[S1]

$$\bar{G} \equiv \frac{G_s(\mu_s/\omega_s) I_s(0) + G_d(\mu_d/\omega_d) I_d(0)}{(\mu_s/\omega_s) I_s(0) + (\mu_d/\omega_d) I_d(0)}. \tag{S23}$$

We found that the solution of the differential equation (S22) is given as [S1]

$$\Delta I_p(z)=\frac{I_p(0)\left\{\frac{\mu_s G_s I_s(0)}{\omega_s}+\frac{\mu_d G_d I_d(0)}{\omega_d}\right\}\left(\exp\left[-\left(\frac{\mu_s V G_s I_s(0)}{\hbar\omega_s c}+\frac{\mu_d V G_d I_d(0)}{\hbar\omega_d c}+\frac{\mu_p V\bar{G} I_p(0)}{\hbar\omega_p c}\right)z\right]-1\right)}{\left\{\frac{\mu_s G_s I_s(0)}{\omega_s}+\frac{\mu_d G_d I_d(0)}{\omega_d}\right\}+\frac{\mu_p \bar{G} I_p(0)}{\omega_p}\exp\left[-\left(\frac{\mu_s V G_s I_s(0)}{\hbar\omega_s c}+\frac{\mu_d V G_d I_d(0)}{\hbar\omega_d c}+\frac{\mu_p V\bar{G} I_p(0)}{\hbar\omega_p c}\right)z\right]}$$

(S24)

In the present case that the depletion beam intensity is much stronger than the pump beam intensity, we can assume the following inequality,

$$\left\{\frac{\mu_s G_s I_s(0)}{\omega_s}+\frac{\mu_d G_d I_d(0)}{\omega_d}\right\}\gg\frac{\mu_p \bar{G} I_p(0)}{\omega_p}\exp\left[-\left(\frac{\mu_s V G_s I_s(0)}{\hbar\omega_s c}+\frac{\mu_d V G_d I_d(0)}{\hbar\omega_d c}+\frac{\mu_p V\bar{G} I_p(0)}{\hbar\omega_p c}\right)z\right].$$

(S25)

Thus, the net intensity change of the pump beam due to the double SRS process is simplified as

$$\Delta I_p(z)=I_p(0)\left(\exp\left[-\left(\frac{\mu_s V G_s I_s(0)}{\hbar\omega_s c}+\frac{\mu_d V G_d I_d(0)}{\hbar\omega_d c}+\frac{\mu_p V\bar{G} I_p(0)}{\hbar\omega_p c}\right)z\right]-1\right). \quad \text{(S26)}$$

For the sake of direct comparison with experimental results on the total pump beam intensity, Eq.(S26) can be rewritten as

$$I_p(z)=I_p(0)+\Delta I_p(z)=I_p(0)\exp\left[-\left(\frac{\mu_s V G_s I_s(0)}{\hbar\omega_s c}+\frac{\mu_d V G_d I_d(0)}{\hbar\omega_d c}+\frac{\mu_p V\bar{G} I_p(0)}{\hbar\omega_p c}\right)z\right]. \quad \text{(S27)}$$

This clearly shows that the total pump intensity decreases exponentially with respect to the depletion beam intensity and the decay constant is $\mu_d V G_d/(\hbar\omega_d c)$. Interestingly, the pump beam intensity decreases upon increasing any of the three beam intensities.

The Raman loss of the pump beam (Fig. 4c) decreases much faster with respect to the depletion beam intensity than the Stokes gain signal intensity does (Fig. 3b). This experimental observation can be understood by examining the theoretical results in Eqs.(S16) and (S27). From Eq.(S16), in the weak Stokes beam intensity region, the Stokes gain signal approximately depends on the depletion beam intensity linearly, i.e.,

$$\Delta I_s(z)\approx c-aI_d(0), \quad \text{(S28)}$$

where the two constants c and a are found to be

$$c=\frac{G_s\mu_pV}{\hbar\omega_pc}I_p(0)I_s(0)z,$$

$$a=\left(\frac{G_s}{G_d}\right)\left(\frac{\mu_d}{\mu_p}\right)\left(\frac{1}{\hbar\omega_dc}\right)\left\{\hbar\omega_pc-\mu_pG_dVz+\hbar c\omega_pe^{\frac{G_dz\mu_pV}{\hbar\omega_pc}I_p(0)}\right\}. \tag{S29}$$

Now, considering the Taylor expansion of the exponential term in Eq.(S27) and taking into account the first-order term, one can find that the Raman pump intensity depends on the depletion beam intensity as,

$$I_p(z)=C-\frac{\mu_dVz}{\hbar\omega_dc}G_d\exp\left[-\left(\frac{\mu_sVG_sI_s(0)}{\hbar\omega_sc}+\frac{\mu_pV\bar{G}I_p(0)}{\hbar\omega_pc}\right)z\right]I_p(0)I_d(0), \tag{S30}$$

where the constant C is given as

$$C=\exp\left[-\left(\frac{\mu_sVG_sI_s(0)}{\hbar\omega_sc}+\frac{\mu_pV\bar{G}I_p(0)}{\hbar\omega_pc}\right)z\right]I_p(0) \tag{S31}$$

Comparing the linear coefficients in the second terms on the right-hand sides of Eqs.(S28) and (S29), we find that the decreasing rates of the Stokes gain signal and the Raman pump intensity loss with respect to the depletion beam intensity are clearly different and the latter (Raman pump loss) depends on the incident depletion beam intensity ($I_d(0)$) much more strongly than the former (Stokes gain). Thus, the experimental results are fully consistent with our theoretical prediction.

III. Numerical calculation of ξ value

The dimensionless coordinate ξ is defined as $\xi=G_dn_p(0)z$. We considered n_p as the pump photon number per pulse, and z as the converted FWHM of the pulse duration in length unit. The pump pulse intensity integrated per unit time and unit volume can be expressed as[S6]

$$I_p^0=E_p^0\frac{8(\ln 2)^{3/2}}{\pi^{3/2}d_p^2\tau_p}, \tag{S32}$$

where τ_p is the pump pulse duration (FWHM), d_p is the focused pump beam diameter at the sample and E_p^0 is the experimentally measured pulse energy. The pump photon number per unit volume can be obtained from the calculated pump pulse intensity. The volume used in this calculation is total interaction volume of one pulse, and calculated as cylinder whose diameter and length are the focused beam diameter and the z value, respectively. We could also calculate G_d by converting the Raman gain coefficient to constant using Eqs.(S4) and (S5).

IV. Experimental Methods

For three-beam double SRS experiments, we used three colored laser beams: 1 ps Raman pump pulse, 100 fs Stokes pulse, and 1 ps depletion pulse. In the present proof-of-principle experiment, we considered two strong Raman-active modes that are the ring breathing mode at 992 cm^{-1} and the C-H stretch mode at 3062 cm^{-1} (Fig. 1d). The frequency difference between the pump and Stokes beams is controlled to be matched to the benzene ring breathing mode (992 cm^{-1}), and the frequency difference between the pump and depletion beams is tuned with the C-H stretch mode (3062 cm^{-1}), leading to two competitive SRS processes. On the other hand, the Stokes and depletion beams do not induce any SRS process because their frequency difference is about 2064 cm^{-1} and there is no Raman mode of benzene at this frequency (Fig. 1d). Liquid benzene was purchased from Sigma-Aldrich and used without any further purification. The liquid sample was placed in a 1-mm-thick glass cuvette (Starna scientific) for subsequent double SRS experiments.

Fig. 2 shows our three-beam double SRS experimental setup with the ps Raman pump (781 nm), fs Stokes (850 nm) and ps depletion (1026.5 nm) beams. Our laser source consists of a Ytterbium-based (Yb:KGW) femtosecond regenerative amplifier (PHAROS; Light Conversion) and two optical parametric amplifiers (OPA) that are pumped by the PHAROS and independently tunable. The laser repetition rate is variable from 1 to 100 kHz, and was fixed to 50 Hz for our experiments. Portions of the fundamental output (1030 nm, ~200 fs) from the regenerative amplifier were used to pump the two OPA's: collinear OPA (COPA, ORPHEUS; Light Conversion) and non-collinear OPA (NOPA, ORPHEUS-N; Light Conversion). Tunable beams from the COPA and NOPA were used as Raman pump and Stokes beams, the center wavelengths of which are 781 nm (bandwidth: $\Delta\lambda$~6 nm) and 850 nm ($\Delta\lambda$>50 nm), respectively. A residual of the fundamental output (1030 nm, $\Delta\lambda$~8nm) was used as depletion beam.

To improve the frequency resolution, we used narrow bandpass filters (NBF) for the pump and depletion beams. By combining a pair of NBFs for each beam, we could narrow the bandwidth down to <1 nm. More specifically, a pair of NBF (LL01-785; Semrock) was used to carve out the bandwidth of 16 cm^{-1} for the pump beam centered at 781 nm. A pair of different NBFs (LL01-

1030-25; Semrock) narrowed the depletion bandwidth down to 14 cm^{-1} centered at 1026.5 nm. On the other hand, the bandwidth of the Stokes beam was controlled to be 250 cm^{-1} (>100 fs), which is the observable frequency window of our experimental setup, using a broad bandpass filter (FF01-850/10; Semrock) to avoid any undesired nonlinear effect, otherwise readily produced by the ultrashort Stokes beam itself (~30 fs). To verify that the center wavelength of the depletion beam is exactly tuned to the C-H stretch mode of benzene, we monitored the resonant CARS signal around 630 nm, which is effectively produced only when the frequency difference (Ω) between the pump (781 nm) and deletion (1026.5 nm) beams is resonant with that vibrational frequency (ω_v = 3063 cm^{-1}), and adjusted the depletion beam wavelength to maximize the resonant CARS signal based on the fact that the vibrationally resonant CARS signal is in general much larger than the non-resonant CARS that is created when $\Omega \neq \omega_v$.

Before the three beams are combined for subsequent double SRS measurements, the pump and Stokes beams were allowed to pass through a home-built spatial filter to improve the spatial beam mode. The spatial filter for the Stokes beam consists of a pinhole (diameter: *d*=30 μm) and two identical lenses (focal length: f=100 mm). For the pump beam, on the other hand, a 1.5:1 telescope with a set of a pinhole (diameter: *d*=25 μm) and two lenses (f=150, 100 mm) was used to reduce the beam size of the pump slightly larger than that of the Stokes beam for better mode-matching with the Stokes beam at the sample. The beam diameters of both beams at the front objective lens were then set to be approximately half of the rear aperture size (15 mm) of the objective lens.

The three beams were combined with dichroic mirrors (DM, #86-694; Edmund, #69-872; Edmund) and then focused at the sample by using a 10X objective lens with NA 0.30 (Plan Fluor; Nikon). A 4X objective lens with NA 0.13 (Plan Fluor; Nikon) was used after the sample to collect the transmitted beams. All the beams were sent to the monochromator (SpectraPro 2300i; Princeton Instruments) equipped with a CCD (DU401-BV; Andor) with 26 × 26 μm pixels for spectral analyses. For the SRS measurement at the Stokes frequency, the depletion and pump beams were blocked by a short pass filter (SPF, #64-332; Edmund) and a notch filter (NF, #86-122; Edmund). For the depletion beam intensity-dependent measurements, the SRS spectra generated by the pump and Stokes pulse pair were recorded by varying the energy of the depletion beam from 0 to 250 nJ with a neutral density filter (ND), which allowed us to study the effect of the depletion beam on the Stokes SRS signal as well as the pump beam intensity. Note that the pulse peak intensity, which is defined as the energy per unit time and per unit area, is proportional to the pulse energy because the pulse width (time) and beam size (area) of the depletion beam at the focal point are kept constant throughout the measurements. The SRS spectra and all the experimental data presented in this paper were measured under the best beam overlap condition, which was guaranteed by maximizing the 3-color CARS signal generated only when all the three beams overlap in time and space.

We obtained the Stokes spectra with and without pump by taking averages over 5000 spectra for each case (Fig. S1a). The two Stokes spectra ($I_{\text{pump-on}}(\omega)$, $I_{\text{pump-off}}(\omega)$) with and without the pump were taken to calculate their ratio, which yields a SRS spectrum ($I_{Gain}(\omega)$, see Fig. S1b for an example),

$$I_{Gain}(\omega) = \frac{I_{pump-on}(\omega)}{I_{pump-off}(\omega)}. \tag{S33}$$

The pump beam was modulated with an optical chopper (MC2000B, MC1F10; Thorlabs) that is synchronized with half (25Hz) of the laser repetition rate (50 Hz). The Stokes pulse spectra when the pump pulse alternately switches on and off were then recorded with the above CCD spectrometer, which is also externally synchronized with the laser system (50 Hz). The background signal originating from laser fluctuation was corrected by subtracting a factor to each spectrum to match the baselines.

Supporting Figures

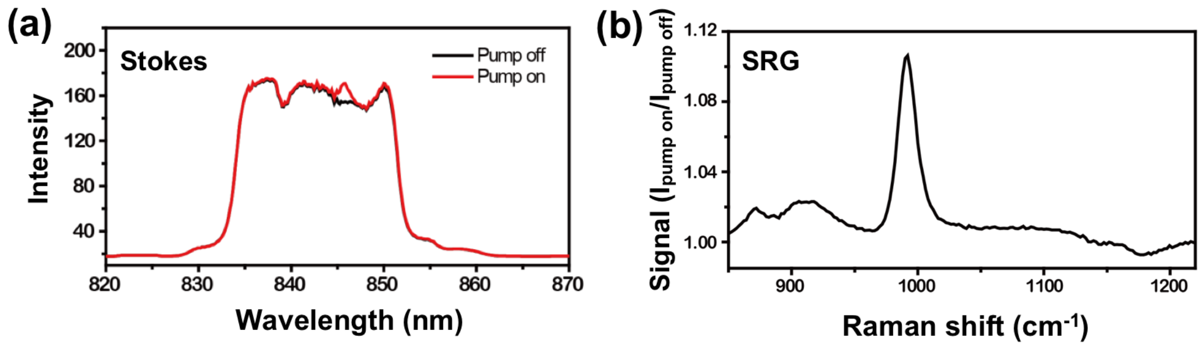

Figure S1. Stokes and SR gain spectra without depletion beam. (a) Spectra of Stokes beam with pump on (red) and off (black) modulation. (b) A stimulated Raman gain spectrum obtained by dividing the Stokes spectra ($I_{pump\_on} / I_{pump\_off}$).

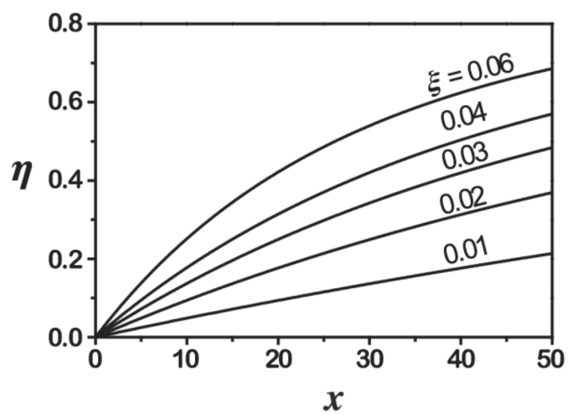

Figure S2. Numerical calculation results for the suppression efficiency in Eq.(S20).

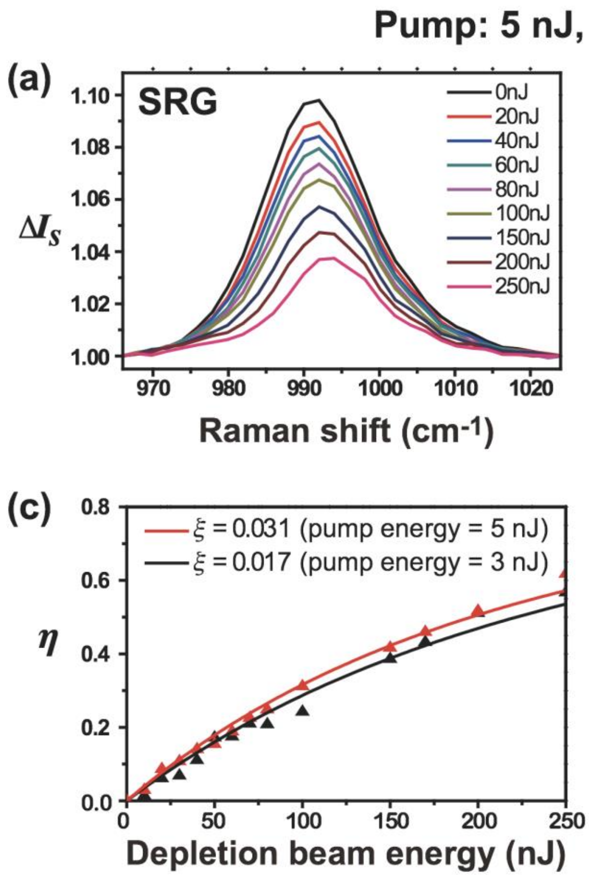

Figure S3. Stimulated Raman gain with depletion light at an increased pump energy (5 nJ). (a) SR gain spectra with 0-250nJ depletion pulse. The pump pulse energy and the Stokes pulse energy are fixed at 5 and 0.8 nJ, respectively. (b) The peak intensities (black squares) of the SRS spectra in (a) are plotted with respect to x ($= n_d(0)/n_p(0)$). Experimentally measured suppression efficiencies (red triangles) are plotted with respect to x. The fit curve with Eq.(S20) is also shown here as a red solid line, where the fit parameter ξ is found to be 0.031. (c) Comparison of suppression efficiency for two pump energy conditions. Each curve indicates the fitting data of suppression efficiency η with 3 nJ pump energy (black) and 5 nJ pump energy (red). Energy condition of other beams is the same except for pump energy.

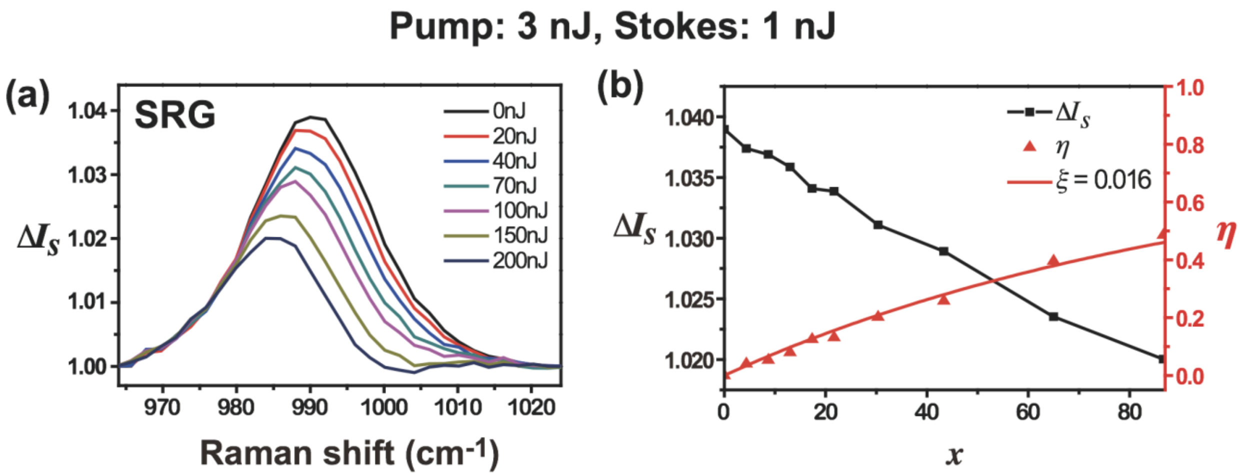

Figure S4. Stimulated Raman gain spectra obtained with an increased Stokes energy (1.0 nJ). (a) The SR gain spectra are plotted for varying depletion pulse energy from 0 to 250 nJ, where the pump pulse energy is 3 nJ and the Stokes pulse energy is 1.0 nJ. (b) The peak intensities (black squares) of the SRS spectra in (a) are plotted with respect to x ($= n_d(0)/n_p(0)$). Experimentally measured suppression efficiencies (red triangles) are plotted with respect to x. The fit curve with Eq.(S20) is also shown here, where the fit parameter ξ is found to be 0.016.

Supplementary References

(S1) Cho, M. Three-Beam Double Stimulated Raman Scatterings. *J. Chem. Phys.* **2017**, submitted.

(S2) Penzkofer, A.; Laubereau, A.; Kaiser, W. High intensity Raman interactions. *Prog. Quant. Electron.* **1979**, *6*, 55-140, DOI: https://doi.org/10.1016/0079-6727(79)90011-9.

(S3) Boyd, R. W., *Nonlinear Optics, 3rd Edition*; Academic Press, 2008.

(S4) Lu, F.-K.; Ji, M.; Fu, D.; Ni, X.; Freudiger, C. W.; Holtom, G.; Xie, S. X. Multicolor stimulated Raman scattering microscopy. *Mol. Phys.* **2012**, *110*, 1927-1932, DOI:10.1080/00268976.2012.695028.

(S5) Yang, W.; Li, A.; Suo, Y.; Lu, F.-K.; Xie, S. X. Simultaneous two-color stimulated Raman scattering microscopy by adding a fiber amplifier to a 2 ps OPO-based SRS microscope. *Opt. Lett.* **2017**, *42*, 523, DOI:10.1364/OL.42.000523.

(S6) Ekvall, K.; Meulen, P. v. d.; Dhollande, C.; Berg, L.-E.; Pommeret, S.; Naskrecki, R.; Mialocq, J.-C. Cross phase modulation artifact in liquid phase transient absorption spectroscopy. *J. Appl. Phys.* **2000**, *87*, 2340-2352, DOI:10.1063/1.372185.